Fluconazole binding and sterol demethylation in three CYP51 isoforms indicate differences in active site topology

Aouatef Bellamine,[1] Galina I. Lepesheva, and Michael R. Waterman

Department of Biochemistry, Vanderbilt University School of Medicine, Nashville, TN 37232-0146

Abstract **14α-Demethylase (CYP51) is a key enzyme in all sterol biosynthetic pathways (animals, fungi, plants, protists, and some bacteria), catalyzing the removal of the C-14 methyl group following cyclization of squalene. Based on mutations found in CYP51 genes from *Candida albicans* azole-resistant isolates obtained after fluconazole treatment of fungal infections, and using site-directed mutagenesis, we have found that fluconazole binding and substrate metabolism vary among three different CYP51 isoforms: human, fungal, and mycobacterial. In *C. albicans*, the Y132H mutant from isolates shows no effect on fluconazole binding, whereas the F145L mutant results in a 5-fold increase in its IC_{50} for fluconazole, suggesting that F145 (conserved only in fungal 14α-demethylases) interacts with this azole. In *C. albicans*, F145L accounts, in part, for the difference in fluconazole sensitivity reported between mammals and fungi, providing a basis for treatment of fungal infections. The *C. albicans* Y132H and human Y145H CYP51 mutants show essentially no effect on substrate metabolism, but the *Mycobacterium tuberculosis* F89H CYP51 mutant loses both its substrate binding and metabolism. Because these three residues align in the three isoforms, the results indicate that their active sites contain important structural differences, and further emphasize that fluconazole and substrate binding are uncoupled properties.**—Bellamine, A, G. I. Lepesheva, and M. R. Waterman. **Fluconazole binding and sterol demethylation in three CYP51 isoforms indicate differences in active site topology. *J. Lipid Res.* 2004.** 45: **2000–2007.**

Supplementary key words *Candida albicans,* human • inhibitor binding • *Mycobacterium tuberculosis* • substrate metabolism

Sterol 14α-demethylases (14DM) belong to a cytochrome P450 family (CYP51) catalyzing removal of a methyl group at position C14 in the sterol molecule (1). This is a key step in cholesterol, ergosterol, and phytosterol synthesis in animals, fungi, and plants (2). 14DM has also been found in mycobacteria and in *Methylococcus capsulatus*, where the reconstituted enzyme was found to convert sterols to their C14-demethylated products (3–5). Isoforms of 14DM from different kingdoms use very closely related sterol molecules as substrate; no other substrate molecules are known. Furthermore, mammalian and fungal forms show differences in their ability to bind azole molecules known to inhibit cytochrome P450 activities (6, 7). For example, fungal 14DMs bind fluconazole several orders of magnitude more tightly than mammalian isoforms, which was the basis for the design of azole inhibitors targeting fungal 14DM versus the human form (8). Inhibition of 14DM activity is lethal in fungi (9); however, treatment by fungistatic azole compounds leads to the emergence of resistant clinical isolates over time.

Several mechanisms involved in such resistance have been elucidated. Overexpression of efflux pumps results in decreased azole availability in the cells at the 14DM target site (10, 11). A second way to counter deficiency in ergosterol availability is the ability of some isolates to use 14-methylated precursors such as 14-methylfecosterol for the sparking hormonal function observed with ergosterol (12). In this case, accumulation of 14α-methyl-ergosta-8,24(28)-dien-3β,6α-diol, an ergosterol 14-methyl precursor, indicates that the azole resistance is caused by loss of sterol 14α-demethylase activity (12). Finally, decreased affinity of 14DM for azole molecules is another cause of azole resistance. In this case, mutations in the CYP51 gene have been identified in some azole-resistant strains (13–15). DUMC136, a *Candida albicans* (CA) drug-resistant strain, is homozygous for multiple mutations in its CYP51 gene (16) and is one of the most extensively studied azole-resistant isolates (16, 17). Compared with an azole-susceptible heterozygous strain ATCC 90028, DUMC136 showed a

Manuscript received 21 June 2004 and in revised form 9 August 2004.

Published, JLR Papers in Press, August 16, 2004.
DOI 10.1194/jlr.M400239-JLR200

Abbreviations: 14DM/CYP51, cytochrome P450 sterol 14α-demethylase; 24M-DHL, 24-methylene dihydrolanosterol; ATCC, American Type Culture Collection; CA, *Candida albicans*; DHL, 24,25-dihydrolanosterol; DLPC, dilauryl-L-α-phosphatidylcholine; H, human; MT, *Mycobacterium tuberculosis.*

[1] To whom correspondence should be addressed.
e-mail: aouatef.bellamine@vanderbilt.edu

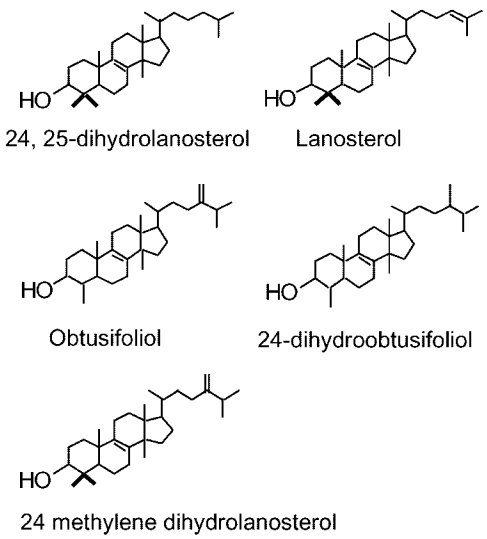

Fig. 1. Sterol structures referred to in this report.

125-fold increase in its minimal fluconazole inhibitory concentration for ergosterol biosynthesis in whole cells (16). The CYP51 gene alleles have two nucleotide substitutions compared to an allelic variant (ATCC 90028-2) of the fluconazole-susceptible strain ATCC 90028, resulting in two amino acid changes: Y132H and F145L. When IC_{50} values were determined for CA 14DM in microsomal fractions, DUMC136 14DM showed only a 10-fold increase in its resistance to fluconazole compared with the IC_{50} from ATCC 90028 or the wild-type strain, without change in 14α-demethylase activity (16). When the single substitution Y132H was reproduced in CA 14DM and expressed in *Saccharomyces cerevisiae*, an increase in the IC_{50} value for fluconazole (12-fold compared with the wild type) was observed without any effect on the enzymatic activity (17). This and subsequent studies clearly show that fluconazole binding and substrate metabolism are uncoupled events.

To better understand the molecular basis of fluconazole resistance and to begin explaining the differences seen in fluconazole inhibition among various 14α-demethylase isoforms (8), we used site-directed mutagenesis to reproduce substitutions Y132H and F145L in CA 14DM as found in the DUMC136 and other clinical isolates and compared their effect on fluconazole binding and substrate metabolism to their corresponding human and *Mycobacterium tuberculosis* (MT) 14DM orthologues. We found that the CA 14DM F145L mutant but not Y132H is responsible for the increase in fluconazole resistance, suggesting that in CA 14DM F145 interacts with the azole. Although CA and human mutations did not notably affect catalytic activity, MT 14DM F89H mutant corresponding to Y132H in CA 14DM completely abolished enzymatic activity and profoundly altered substrate binding, indicating a role of MT 14DM F89 in substrate binding. These results indicate that the topology in the active sites of the CYP51 isoforms is different even though all three enzymes serve the same function and metabolize the same substrates.

MATERIALS AND METHODS

General methods

Flavodoxin, flavodoxin reductase, and rat P450 reductase were kindly provided by Dr. Chris Jenkins (18, 19). The 24,25-[24-^{3}H] dihydrolanosterol was a generous gift from Dr. James Trzaskos. The 24,25-dihydrolanosterol (DHL), lanosterol, 24-methylene dihydrolanosterol (24M-DHL), obtusifoliol, and 24-dihydroobtusifoliol (**Fig. 1**) were kindly provided by Dr. David Nes. The fluconazole was a generous gift from Pfizer. The Triton X-114 (Fluka Chemical, Ronkonkoma, NY) was purified as described (20) before use in protein purification. Sequence alignment was performed using Clustalw 1.81 software (European Bioinformatics Institute website) and prepared in εSprit 2.1 programs (http://genopole.toulouse.fr).

Mutant construction

Primer sequences used for mutagenesis were represented in **Table 1** and MT 14 DM/pET-17b (3) was the template for MT 14DM mutants. To construct the H Y145H/pCWOri+ expression vector, the *Nco*I/*Spe*I fragment (659 bp) of wild-type H 14DM/pCWOri+ (21) is exchanged with the corresponding fragment of mutated DNA in clone 14B (21). To construct the CA 14DM Y132H/pCWOri+ and F145L/pCWOri+ mutants, the *Sac*I/*Spe*I fragment (1,091 bp) of CA 14DM/pCWOri+ wild type (22) is exchanged with the mutated DNA in pBSIIKS (Stromstedt, personal communication). To construct CA 14DM Y132H/F145L/pCWOri+, CA 14DM Y132H/pBSIIKS previously constructed was used as template in combination with primers used

TABLE 1. Primers used for mutagenesis

Mutants and Corresponding Residue Changes	Primer Sequences
MT 14DM F89H	5′-cggcgagggcgtggtgt(c)t(a)cgacgccagcccggaacgg-3′
	5′-ccgttccgggctggcgtcga(t)a(g)caccacgccctcgccg-3′
MT 14DM F89Y	5′-cggcgagggcgtggtgtt(a)cgacgccagcccggaacgg-3′
	5′-ccgttccgggctggcgtcga(t)acaccacgccctcgccg-3′
MT 14DM F89A	5′-cggcgagggcgtggtgt(g)t(c)cgacgccagcccggaacgg-3′
	5′-ccgttccgggctggcgtcga(g)t(c)caccacgccctcgccg-3′
H 14DM Y143H	5′-gggaagggagttgcac(t)acgatgtgcctaatcc-3′
	5′-ggattaggcacatcgtg(a)tgcaactccctccc-3′
CA 14DM Y132H	5′-ggtaaaggggttattt(c)atgattgtccaaattcc-3′
	5′-ggaatttggacaatcata(g)aataacccctttacc-3′
CA 14DM F145L	5′-ggaacaaaaaaaat(c)ttgctaaatttgc-3′
	5′-gcaaatttagcaaa(g)ttttttttgttcc-3′

Primers design based on the MT 14DM coding sequence (GenBank accession no. MTCY369), with mutated bases shown in parentheses.

for CA F145L mutagenesis (Table 1) and the *Sac*I/*Spe*I fragment (1,091 bp) of CA 14DM/pCWOri+ is exchanged with the mutated DNA. Mutagenesis is performed using QuikChange™ Site-Directed Mutagenesis Kit according to the conditions of the manufacturer (Stratagene, La Jolla, CA). The full coding region of MT mutants and the mutated fragments of CA and human mutants were sequenced using automated sequencing: Applied Biosystems PRISM Big Dye Terminator Cycle Sequencing Ready Reaction kit and Applied Biosystems PRISM 377 DNA sequencer (ABI, Foster City, CA).

P450 expression and purification

MT 14DM and its mutants were expressed and purified as described (3), except that a Q Sepharose High Performance column (Amersham Pharmacia Biotech, Piscataway, NJ) was used instead of the HQ column on the HPLC. Both the wild type and the mutants were eluted at 190 to 250 mM NaCl concentration. Fractions corresponding to a 417nm/280nm ratio of 1.4 and higher were pooled and P450s were dialyzed against 0.1 M Tris-HCl, pH 7.5/0.1 mM EDTA/20% glycerol. Human and CA 14DMs and their mutants were expressed in the HMS174 *Escherichia coli* strain (Novagen, Madison, WI) and purified as described for H 14DM except that lanosterol and ketoconazole were omitted from the buffer (23). P450s were dialyzed against 20 mM Tris-HCl, pH 7.5/0.1 mM EDTA/20% glycerol/0.1% Triton X-100 (Boehringer Mannheim, Indianapolis, IN) (buffer B) and loaded onto a Hydroxyapatite Bio-Gel® HTP Gel column (Bio-Rad, Hercules, CA) for further purification. The column was washed with buffer B and P450 eluted using 0–400 mM potassium phosphate pH 7.5 and a 0–0.4% Triton X-100 gradient. Fractions corresponding to 50–100 mM potassium phosphate were pooled and dialyzed against buffer B.

P450 reconstituted activity

One nanomole of MT 14DM, F89H or F89Y mutants was incubated on ice with 18 nmol of *E. coli* flavodoxin and 2 nmol of *E. coli* flavodoxin reductase. After 10 min, 25 nmol of DHL/[24-^{3}H]DHL dispersed in Triton WR 1339 (16 mg/ml) (SERVA, Hauppauge, NY) (21), 0.4 mg/ml of isocitrate dehydrogenase, 25 mM sodium isocitrate (Sigma-Aldrich, St. Louis, MO), and 100 μl of buffer (100 mM MOPS, pH 7.5; 250 mM KCl; 25 mM $MgCl_2$; 50% glycerol) and water was added to 500 μl volume. The reaction mixture was preincubated for 2 min at 37°C before adding NADPH (Calbiochem, La Jolla, CA) to 5 mM. Aliquots were collected after 10, 20, and 60 min. Sterols were extracted and analyzed by HPLC as described (21). For H 14DM, CA 14DM, and

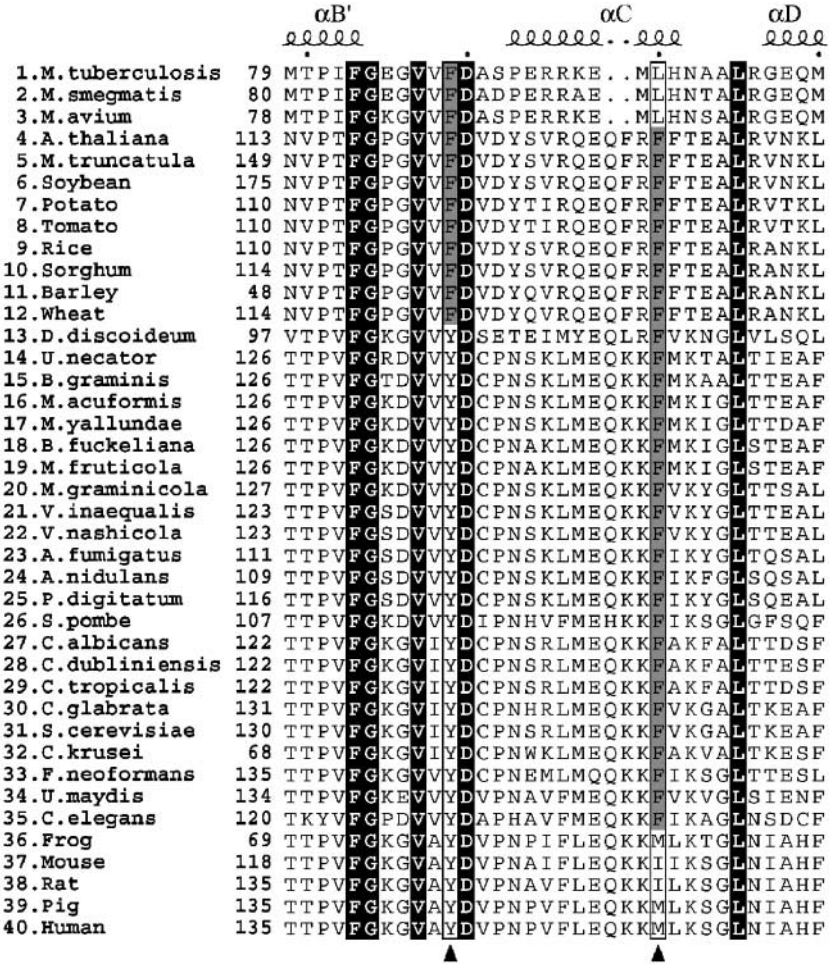

Fig. 2. 14α-demethylase sequence alignment. Sequences of 40 14α-demethylases (14DM) were aligned using Clustalw 1.81 software. Numbering of the residues starts from the first methionine (start codon) when the N-terminal sequence is known. Arrow heads indicate residues Y132 and F145 of CA 14DM. Residues completely conserved are included in black boxes. MT 14DM secondary elements are represented above the MT 14DM primary sequence.

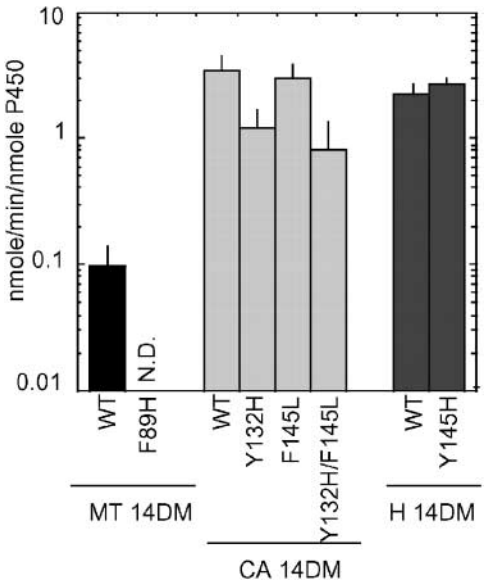

Fig. 3. 24,25-Dihydrolanosterol (DHL) metabolism. Turn-over numbers determined for CA, human, and MT 14DMs and their mutants using DHL as substrate are expressed as nmol of product/min/nmol of P450 (log scale). N.D., no detectable activity. Error bars represent standard deviation.

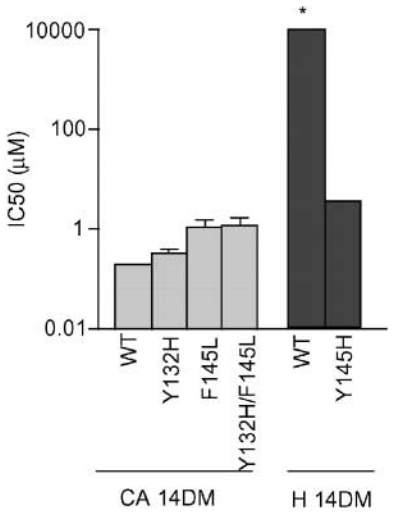

Fig. 5. IC_{50} determination. Fluconazole inhibition of CA 14DM, H 14DM and mutant activities based on IC_{50} (μM). Values are determined for 50 μM DHL conversion at 37°C in presence of increasing concentrations of fluconazole and expressed as the percent of activity with fluconazole versus activity without fluconazole (log scale). * Up to 10 mM limit of solubility for fluconazole, H 14DM is still fully active. Error bars represent standard deviation.

their mutants, 1 nmol of P450, 5 nmol of rat P450 reductase and 50 μg of dilauryl-L-α-phosphatidylcholine (DLPC) were used. After addition of 25 nmol of DHL/[24-^{3}H]DHL and incubation on ice, reactions were performed as described for MT 14DM and stopped at 5, 10, 20, and 60 min. For the IC_{50} determinations, reactions were performed in the presence of increasing concentrations of fluconazole: 0, 0.25, 0.5, 2, and 4 μM for CA 14DM and its mutants; 0, 1, 2, 5, and 10 μM for the H 14DM Y145H mutant and 0, 0.1, 1, 5, and 10 mM for wild-type H 14DM.

Spectral analyses

Sterol binding for MT 14DM and its mutants was performed as described (24). Fluconazole binding was performed as for sterol binding except that P450s were diluted to 5 μM in 1 ml of 20 mM MOPS, pH 7.5/50 mM KCl/5 mM $MgCl_2$/10% glycerol and titrated with 500 nM to 200 μM fluconazole for MT, human 14DMs, and their mutants and with 100 nM to 10 μM fluconazole for CA 14DM and its mutants. Spectra were recorded between 350 nm and 450 nm, revealing changes at 412 nm and 435 nm characteristic of a P450 type II binding spectrum (6). Because fluconazole was dissolved in ethanol, a corresponding volume of solvent was added simultaneously to the P450 chamber of the reference cuvette and the buffer chamber of the sample cuvette. The same results were obtained using DMSO.

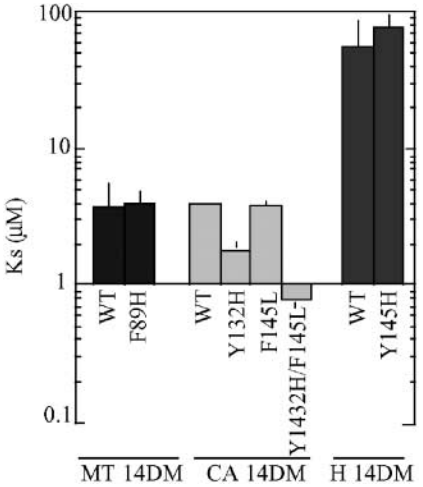

Fig. 4. Fluconazole binding. Fluconazole binding of *Mycobacterium tuberculosis* (MT), *Candida albicans* (CA), and human (H) 14DMs and their mutants based on type II binding spectra. K_s values (μM) are shown as log scale. Error bars represent standard deviation.

RESULTS

Conservation of Y132 of *C. albicans* among CYP51s and its role in catalytic activity

A sequence alignment of 40 different 14α-demethylase isoforms shows that the CA 14DM Y132 residue is conserved among fungi and animals and corresponds to Y145 in human 14DM. In plant and bacterial isoforms, this position is occupied by phenylalanine and corresponds to F89 in MT 14DM (**Fig. 2**). Y132, Y145, and F89 in CA, human, and MT 14DMs, respectively, were substituted by histidine as found in CA clinical isolates. F145L also found in CA clinical isolates, occasionally in combination with Y132H, was also reproduced only in the CA 14DM, because this residue is not conserved in the human and MT isoforms. Note that Y145 in human 14DM aligns with Y132 in CA and not F145 (Fig. 2). In *E. coli*, 14DM mutants showed similar P450 expression levels to the corresponding wild types: MT 14DM and F89H mutant were expressed at 800 to 1,200 nmol/l, whereas H 14DM and its mutant were expressed at 200 nmol/l and CA 14DM and its mutants at 100 nmol/l.

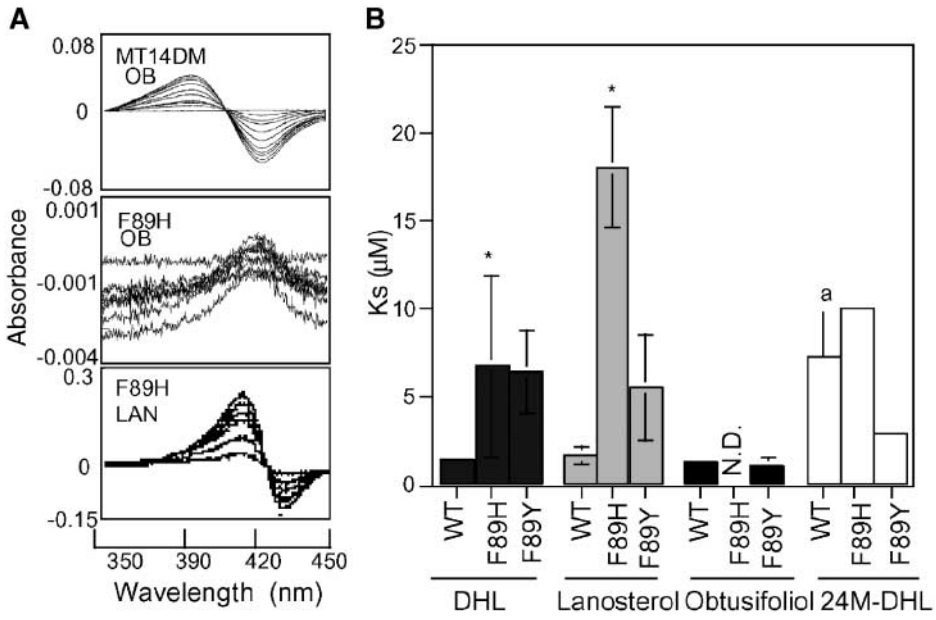

Fig. 6. MT 14DM sterol binding. A: Type I binding spectra for obtusifoliol (OB) are shown for MT 14DM and its mutant F89H and lanosterol (LAN) for F89H. B: K_s values (μM) of MT 14DM and its mutants for DHL, lanosterol, obtusifoliol and 24M-DHL are estimated based on type I binding spectra. * Altered type I binding spectra (see text). N.D., no detectable binding. Error bars represent standard deviation. [a] Value previously determined (24).

Catalytic activities

24,25-Dihydrolanosterol (DHL) (Fig. 1) was used as substrate for both wild-type and mutant forms. CA 14DM Y132H showed a 2-fold decrease in turnover number and F145L did not alter DHL metabolism. Human 14DM Y145H showed no change in turnover, but in MT the 14DM F89H mutant lost catalytic activity (**Fig. 3**). This suggests that in CA and in human 14DMs the Y132 and Y145 residues, respectively, are not required for activity, but that F89 (which aligns with these two) is required in MT 14DM.

Role of CA 14DM mutants in fluconazole binding

Type II binding spectra. P450s were tested for their ability to bind fluconazole based on type II binding spectra (6). CA14DM Y132H mutant was found to have insignificantly higher affinity for fluconazole (2-fold decrease in K_s value) and F145L showed similar K_s value to the CA wild type (**Fig. 4**). Neither H Y145H 14DM nor MT F89H mutants showed any change compared with their respective wild types (Fig. 4). Furthermore, F89H did not alter binding to clotrimazole and ketoconazole, two other P450 azole-inhibitors (data not shown). Because triadimenol treatment of the grape powdery mildew fungus *Uncinula necator* resulted in the appearance of resistant clones, with the fungal CYP51 having Y136F substitution (corresponding to F89 in MT 14DM) (25), we also mutated MT 14DM F89 to tyrosine and found no change in fluconazole binding. This is in agreement with the X-ray structure determination of the fluconazole-bound form of MT 14DM, where F89 did not show interaction with fluconazole (26). These results based on type II binding spectra suggest that Y132 and F145 in CA, Y145 in human and F89 in MT 14DMs are not directly involved in fluconazole binding. However, previous reports indicate that CA 14DM Y132H mutant expressed in *S. cerevisiae* and analyzed in a microsomal fraction led to a 12-fold increase in fluconazole resistance (17). Furthermore, the CA DUMC136 resistant strain (having both Y132H and F145L substitutions in its CYP51 gene) showed a 10-fold increase in its resistance to fluconazole (16). In both latter studies, fluconazole affinity was determined based on IC_{50} and not type II spectra as it is in our study.

Effect of F154L on CA 14DM IC_{50} for fluconazole. Using DHL as substrate, IC_{50} values were determined for CA and human 14DM mutants but not for MT 14DM F89H, because this mutant has no catalytic activity. The IC_{50} determination showed no change in fluconazole resistance for the CA 14DM Y132H mutant. However, both the CA 14DM F145L and Y132H/F145L mutants showed significant increase in their IC_{50} values for fluconazole (about 5-fold) (**Fig. 5**), suggesting that F145L substitution but not Y132H is responsible for the observed fluconazole resistance in the clinical isolates. Surprisingly, the human Y145H mutant that corresponds to Y132H in CA 14DM showed a decrease of more than three orders of magnitude in its IC_{50} value, compared with the wild type (Fig. 5), suggesting a much higher affinity for fluconazole for this mutant and implying that a histidine at position 145 interacts with fluconazole in the human isoform. The difference seen between IC_{50} and K_s values (Figs. 5, 6) implies that interaction of fluconazole with CA and human 14DMs is

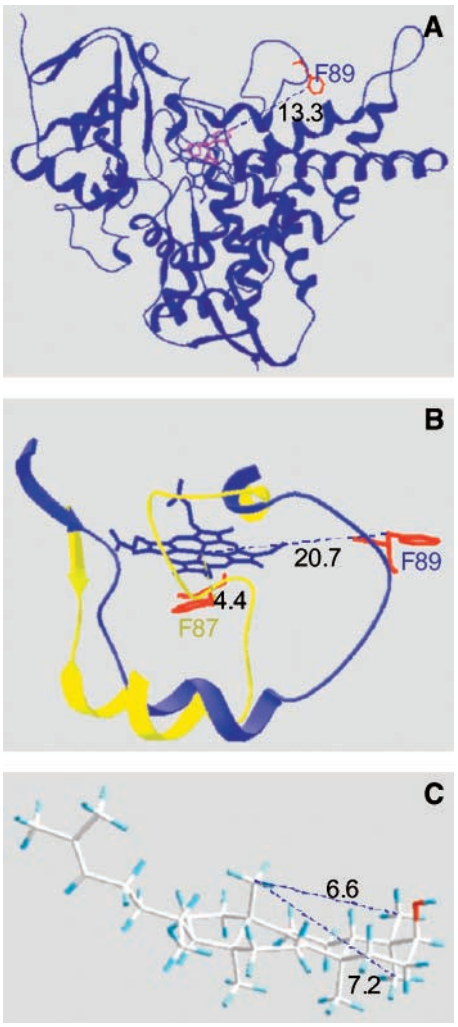

Fig. 7. MT 14DM/sterol interaction. A: Overall view of MT CYP51 crystal structure in complex with fluconazole (purple) and its distance to F89 (red). B: MT 14DM (blue) and BM3 (yellow) structures are superposed in their B-C loop regions and the relative distances of MT 14DM F89 (red) and BM3 F87 (red) to the heme center (blue) are shown. C: Distances between the 2 C4- and the C14-methyl groups are shown in the three-dimensional representation of lanosterol.

different when the P450 is oxidized and low spin (type II binding spectrum) than when it is reduced and high spin and in the presence of substrate and P450 reductase (IC_{50} determination). It has been reported that *S. cerevisiae* 14DM interacts differently with azole molecules when the P450 is oxidized or when it is reduced (9).

These results suggest that fluconazole interacts with different residues in CA and human isoforms and that this interaction depends on the P450 oxidation-reduction state and its environment (presence of the substrate, P450 reductase and DLPC). The difference in fluconazole binding seen between human and CA 14DMs (Fig. 5) and reported between mammalian and fungal isoforms (more than five orders of magnitude) (8) might be explained in part by presence of F145 in CA 14DM, absent in the human isoform.

Role of F89 in MT 14DM/substrate binding

Loss of activity of the MT F89H mutant is due to a profound alteration in substrate binding (**Fig. 6**). Indeed, DHL, lanosterol, and 24M-DHL showed altered type I binding spectra, with a shift of the maxima from 390 nm to 412 nm (Fig. 6A). Estimated K_s values for F89H based on spectral changes are significantly higher (about an order of magnitude) for lanosterol and DHL and in the same order of magnitude for 24M-DHL (Fig. 6B), suggesting a lower affinity for these substrates. The F89H mutant has lost any ability to bind obtusifoliol (Fig. 6B) the best substrate for this enzyme (3, 24), or 24-dihydroobtusifoliol (Fig. 1), another C4-monomethyl sterol (data not shown). Because CA Y132 is conserved among mammals and fungi, where this residue does not alter substrate metabolism, we also checked the substrate binding for the MT 14DM F89Y mutant. This mutant showed a moderate decrease (3-fold) in its catalytic activity (data not shown) and slightly decreased affinity for DHL and lanosterol without effect on obtusifoliol binding (Fig. 6B). However, when F89 is mutated to an alanine, the enzyme lost its catalytic activity and its ability to bind obtusifoliol as seen for F89H mutant (data not shown). Obtusifoliol and 24-dihydroobtusifoliol are C4-monomethyl sterols; lanosterol, DHL, and 24M-DHL are C4-dimethyl sterols (Fig. 1). The fact that the F89H and F89A mutants do not bind obtusifoliol and F89H showed altered binding to DHL, lanosterol, and 24M-DHL suggests that the F89 residue in MT 14DM interacts with the sterol molecule at its C4β-methyl group. Interaction between F89H and C4-dimethyl sterols resulting in impaired type I binding spectra without catalytic activity, suggests that another residue in the MT 14DM mutants interacts with the C4α-methyl group resulting in incorrectly positioned C4-dimethyl sterols. F89H and F89A lost their binding to obtusifoliol but F89Y did not, perhaps because an aromatic residue at the position 89 is required for obtusifoliol interaction at its C4β-methyl group.

DISCUSSION

These results imply that both azole and substrate binding are different in each of the three CYP51 isoforms studied. Because the structure of MT 14DM is known, it is the easiest of the three to explain. MT 14DM F89H did not show any effect in fluconazole binding based on type II binding spectrum. Accordingly, crystal-structure determination of the MT 14DM fluconazole-bound form showed no interaction between F89 and fluconazole (26). In CA 14DM, Y132H mutant showed no effect on fluconazole binding but F145L substitution resulted in a 5-fold increase of IC_{50}, a value similar to the one reported for the CA 14DM clone from the DUMC136 isolate (having both Y132H and F145L substitutions) when expressed in *E. coli* (27). This suggests that F145L but not Y132H is responsible for fluconazole resistance. However, when the same clone (having both mutations) is studied in microsomal fractions from CA, the IC_{50} increases by 10-fold (16), a

value closer to the one reported for the single Y132H mutant expressed in *S. cerevisiae* studied also in a microsomal fraction (12-fold) (17). It is possible that the differences in fluconazole sensitivity of CA 14 DM mutants, seen between results using *E. coli* expression (data herein and Ref. 27) and fungal microsomal fractions (16, 17) may be due to differences in the lipid composition (DLPC in the reconstituted system and *E. coli* membranes versus CA and *S. cerevisiae* microsomes). Unexpectedly, the H1 4DM Y145H substitution resulted in a dramatic decrease in the IC_{50} value (three orders of magnitude), suggesting a possible interaction of a histidine at this position with the fluconazole, leading to better positioning of the azole toward the heme center and therefore greater sensitivity for fluconazole of the human Y145H versus CA Y132H during the catalytic cycle.

Another unexpected result was the loss of substrate metabolism and binding for MT 14DM F89H and F89A mutants, although the corresponding mutants in CA and human had no effect on catalytic activity. This suggests that F89 in MT has a critical role in substrate/P450 interaction. Accordingly, systematic mutation in MT 14DM of the conserved F83, G84, and D90 to alanine abolished catalytic activity (28). Although residues F83, G84, D90, and F89 are part of SRS1 (substrate recognition site) defined for 14α-demethylases (29), crystal structure determination of substrate-free MT 14DM suggests that these residues are located in a B-C loop structure at the open surface of a putative access channel, about 20 Å from the heme iron, making interaction with the bound substrate unlikely without a profound conformational change (26) (**Fig. 7A**).

The structure of the substrate-bound form of MT 14DM has not yet been determined, however, because of the highly nonpolar properties of the substrates, so these results are difficult to explain. One possibility is that residues in the SRS1 and B-C loop region interact with the substrate during MT 14DM/substrate recognition and contribute to its orientation at the heme center, an interaction that is lost once the substrate reaches the active site. Another possibility is that MT 14DM/substrate binding induces a closing of the B-C loop, allowing the substrate access to the active site. Thus, the distance between F89 and the heme iron will become shorter and more comparable with the distances separating C4- and C14-methyl groups (Fig. 7A, C). Indeed, the B-C loop region has a high B factor value, reflecting its high mobility (26). In P450 BM3 (CYP102A1), another soluble P450 with known three-dimensional structure, residue F87 also located in the B-C loop region showed different conformations in the absence or presence of the substrate (30). P450 BM3 F87Y and F87G substitutions result in a decreased affinity and turnover numbers, suggesting a critical role for the F87 in substrate binding and product release during the catalytic cycle (31). Although MT 14DM and BM3 B-C loops are not superposed (Fig. 7B), our results showing loss of substrate binding for F89H and F89A mutants and decreased turnover number for F89Y suggest that, in MT 14DM, F89 might play a role similar to that of F87 in P450 BM3 substrate binding. Corresponding residues Y132 and Y145 in CA and human 14 DMs, also located in SRS1, are not critical for substrate metabolism, because the Y132H mutant showed only a slight decrease in CA 14DM catalytic activity and the Y145H mutant showed no alteration on the H 14DM activity. Perhaps the conformational change in soluble CYP51 is more profound than that in CYP51s located in membranes.

In summary, fluconazole interacts with CA F145 conserved in fungi but replaced by a methionine in humans, suggesting that part of the differences in fluconazole sensitivity reported between animal and fungal isoforms (several orders of magnitude) (8) are due to the presence of residue F145 in CA but not in human. The difference seen in substrate binding and metabolism upon mutation of a semiconserved tyrosine substitution (CA Y132H, H Y145H, and MT F89H) reflects structural differences in the active sites in the three CYP51 isoforms also observed in fluconazole binding studies. Even though these enzymes share great catalytic similarity, the proposed structural differences in their active sites are the basis for the design of drugs selectively targeting microbial CYP51s versus the human isoform. Note that fluconazole was designed to selectively inhibit CA CYP51 versus the human isoform in the absence of any structural data for these enzymes, suggesting differences between these isoforms. Based on mutations found in fluconazole-resistant clinical isolates, we have been able to show that these differences are the result of different interaction of selected residues in the three CYP51s studies with the inhibitor and the substrate indicating differences in their active site topologies.

This work was supported by grants GM37942 and ES 00267-32 from the National Institute of Health (to M.R.W.).

REFERENCES

1. Fischer, R. T., S. H. Stam, P. R. Johnson, S. S. Ko, R. L. Magolda, J. L. Gaylor, and J. M. Trzaskos. 1989. Mechanistic studies of lanosterol 14α-methyl demethylase: substrate requirements for the component reactions catalyzed by a single cytochrome P-450 isozyme. *J. Lipid Res.* **30:** 1621–1632.
2. Yoshida, Y. 1993. Sterol biosynthesis. *In* Cytochrome P-450. 2nd edition. T. Omura, Y. Ishimura, and Y. Fujii-Kuriyama, editors. Kodansha, Tokyo. 93–101.
3. Bellamine, A., A. T. Mangla, W. D. Nes, and M. R. Waterman. 1999. Characterization and catalytic properties of the sterol 14α-demethylase from *Mycobacterium tuberculosis*. *Proc. Natl. Acad. Sci. USA.* **96:** 8937–8942.
4. Jackson, C. J., D. C. Lamb, T. H. Marczylo, A. G. Warrilow, N. J. Manning, D. J. Lowe, D. E. Kelly, and S. L. Kelly. 2002. A novel sterol 14α-demethylase/ferredoxin fusion protein (MCCYP51FX) from *Methylococcus capsulatus* represents a new class of the cytochrome P450 superfamily. *J. Biol. Chem.* **277:** 46959–46965.
5. Jackson, C. J., D. C. Lamb, T. H. Marczylo, J. E. Parker, N. L. Manning, D. E. Kelly, and S. L. Kelly. 2003. Conservation and cloning of CYP51: a sterol 14α-demethylase from *Mycobacterium smegmatis*. *Biochem. Biophys. Res. Commun.* **301:** 558–563.
6. Schenkman, J. B., H. Remmer, and R. W. Estabrook. 1967. Spectral studies of drug interaction with hepatic microsomal cytochrome. *Mol. Pharmacol.* **3:** 113–123.
7. Swinney, D. C., O. Y. So, D. M. Watson, P. W. Berry, A. S. Webb, D. J.

Kertesz, E. J. Shelton, P. M. Burton, and K. A. Walker. 1994. Selective inhibition of mammalian lanosterol 14α-demethylase by RS-21607 in vitro and in vivo. *Biochemistry.* **33:** 4702–4713.
8. Aoki, Y., F. Yoshihara, M. Kondoh, Y. Nakamura, N. Nakayama, and M. Arisawa. 1993. Ro 09-1470 is a selective inhibitor of P-450 lanosterol C-14 demethylase of fungi. *Antimicrob. Agents Chemother.* **37:** 2662–2667.
9. Yoshida, Y., and Y. Aoyama. 1991. Sterol 14α-demethylase and its inhibition: structural considerations on interaction of azole antifungal agents with lanosterol 14α-demethylase (P-450(14DM)) of yeast. *Biochem. Soc. Trans.* **19:** 778–782.
10. Sanglard, D., K. Kuchler, F. Ischer, J. L. Pagani, M. Monod, and J. Bille. 1995. Mechanisms of resistance to azole antifungal agents in *Candida albicans* isolates from AIDS patients involve specific multidrug transporters. *Antimicrob. Agents Chemother.* **39:** 2378–2386.
11. Kolaczkowski, M., and A. Goffeau. 1997. Active efflux by multidrug transporters as one of the strategies to evade chemotherapy and novel practical implications of yeast pleiotropic drug resistance. *Pharmacol. Ther.* **76:** 219–242.
12. Watson, P. F., M. E. Rose, S. W. Ellis, H. England, and S. L. Kelly. 1989. Defective sterol C5–6 desaturation and azole resistance: a new hypothesis for the mode of action of azole antifungals. *Biochem. Biophys. Res. Commun.* **164:** 1170–1175.
13. Sanglard, D., F. F. Ischer, L. Koymans, and J. Bille. 1998. Amino acid substitutions in the cytochrome P-450 lanosterol 14α-demethylase (CYP51A1) from azole-resistant *Candida albicans* clinical isolates contribute to resistance to azole antifungal agents. *Antimicrob. Agents Chemother.* **42:** 241–253.
14. Lamb, D. C., D. E. Kelly, W. H. Schunck, A. Z. Shyadehi, M. Akhtar, D. J. Lowe, B. C. Baldwin, and S. L. Kelly. 1997. The mutation T315A in *Candida albicans* sterol 14α-demethylase causes reduced enzyme activity and fluconazole resistance through reduced affinity. *J. Biol. Chem.* **272:** 5682–5688.
15. White, T. C. 1997. The presence of an R467K amino acid substitution and loss of allelic variation correlate with an azole-resistant lanosterol 14α demethylase in *Candida albicans*. *Antimicrob. Agents Chemother.* **41:** 1488–1494.
16. Asai, K., N. Tsuchimori, K. Okonogi, J. R. Perfect, O. Gotoh, and Y. Yoshida. 1999. Formation of azole-resistant *Candida albicans* by mutation of sterol 14-demethylase P450. *Antimicrob. Agents Chemother.* **43:** 1163–1169.
17. Kelly, S. L., D. C. Lamb, and D. E. Kelly. 1999. Y132H substitution in *Candida albicans* sterol 14α-demethylase confers fluconazole resistance by preventing binding to haem. *FEMS Microbiol. Lett.* **180:** 171–175.
18. Jenkins, C. M., I. Pikuleva, N. Kagawa, and M. R. Waterman. 1997. *Escherichia coli* flavodoxin sepharose as an affinity resin for cytochromes P450 and use to identify a putative cytochrome P450c17/3β-hydroxysteroid dehydrogenase interaction. *Arch. Biochem. Biophys.* **347:** 93–102.
19. Jenkins, C. M., and M. R. Waterman. 1998. NADPH-flavodoxin reductase and flavodoxin from *Escherichia coli*: characteristics as a soluble microsomal P450 reductase. *Biochemistry.* **37:** 6106–6113.
20. Bordier, C. 1981. Phase separation of integral membrane proteins in Triton X-114 solution. *J. Biol. Chem.* **256:** 1604–1607.
21. Stromstedt, M., D. Rozman, and M. R. Waterman. 1996. The ubiquitously expressed human CYP51 encodes lanosterol 14α-demethylase, a cytochrome P450 whose expression is regulated by oxysterols. *Arch. Biochem. Biophys.* **329:** 73–81.
22. Lepesheva, G. I., L. M. Podust, A. Bellamine, and M. R. Waterman. 2001. Folding requirements are different between sterol 14α-demethylase (CYP51) from *Mycobacterium tuberculosis* and human or fungal orthologs. *J. Biol. Chem.* **276:** 28413–28420.
23. Majdic, G., M. Parvinen, A. Bellamine, H. J. Harwood, Jr., W. W. Ku, M. R. Waterman, and D. Rozman. 2000. Lanosterol 14α-demethylase (CYP51), NADPH-cytochrome P450 reductase and squalene synthase in spermatogenesis: late spermatids of the rat express proteins needed to synthesize the follicular fluid meiosis activating sterol. *J. Endocrinol.* **166:** 463–474.
24. Bellamine, A., A. T. Mangla, A. L. Dennis, W. D. Nes, and M. R. Waterman. 2001. Structural requirements for substrate recognition of *Mycobacterium tuberculosis* 14α-demethylase: implications for sterol biosynthesis. *J. Lipid Res.* **42:** 128–136.
25. Delye, C., F. Laigret, and M. F. Corio-Costet. 1997. A mutation in the 14α-demethylase gene of *Uncinula necator* that correlates with resistance to a sterol biosynthesis inhibitor. *Appl. Environ. Microbiol.* **63:** 2966–2970.
26. Podust, L. M., T. L. Poulos, and M. R. Waterman. 2001. Crystal structure of cytochrome P450 14α-sterol demethylase (CYP51) from *Mycobacterium tuberculosis* in complex with azole inhibitors. *Proc. Natl. Acad. Sci. USA.* **98:** 3068–3073.
27. Aoyama, Y., M. Kudo, K. Asai, K. Okonogi, T. Horiuchi, O. Gotoh, and Y. Yoshida. 2000. Emergence of fluconazole-resistant sterol 14-demethylase P450 (CYP51) in *Candida albicans* is a model demonstrating the diversification mechanism of P450. *Arch. Biochem. Biophys.* **379:** 170–171.
28. Lepesheva, G. I., C. Virus, and M. R. Waterman, M. 2003. Conservation in the CYP51 family: role of the B′ helix/BC loop and helices F and G in enzymatic function. *Biochemistry.* **42:** 9091–9101.
29. Yoshida, Y., M. Noshiro, Y. Aoyama, T. Kawamoto, T. Horiuchi, and O. Gotoh. 1997. Structural and evolutionary studies on sterol 14-demethylase P450 (CYP51), the most conserved P450 monooxygenase: II. Evolutionary analysis of protein and gene structures. *J. Biochem. (Tokyo).* **122:** 1122–1128.
30. Li, H., and T. L. Poulos. 1997. The structure of the cytochrome p450BM-3 haem domain complexed with the fatty acid substrate, palmitoleic acid. *Nat. Struct. Biol.* **4:** 140–146.
31. Noble, M. A., C. S. Miles, S. K. Chapman, D. A. Lysek, and A. C. MacKay. 1999. Roles of key active-site residues in flavocytochrome P450 BM3. *Biochem. J.* **9:** 371–379.